STATE OF THE CLIMATE IN 2012

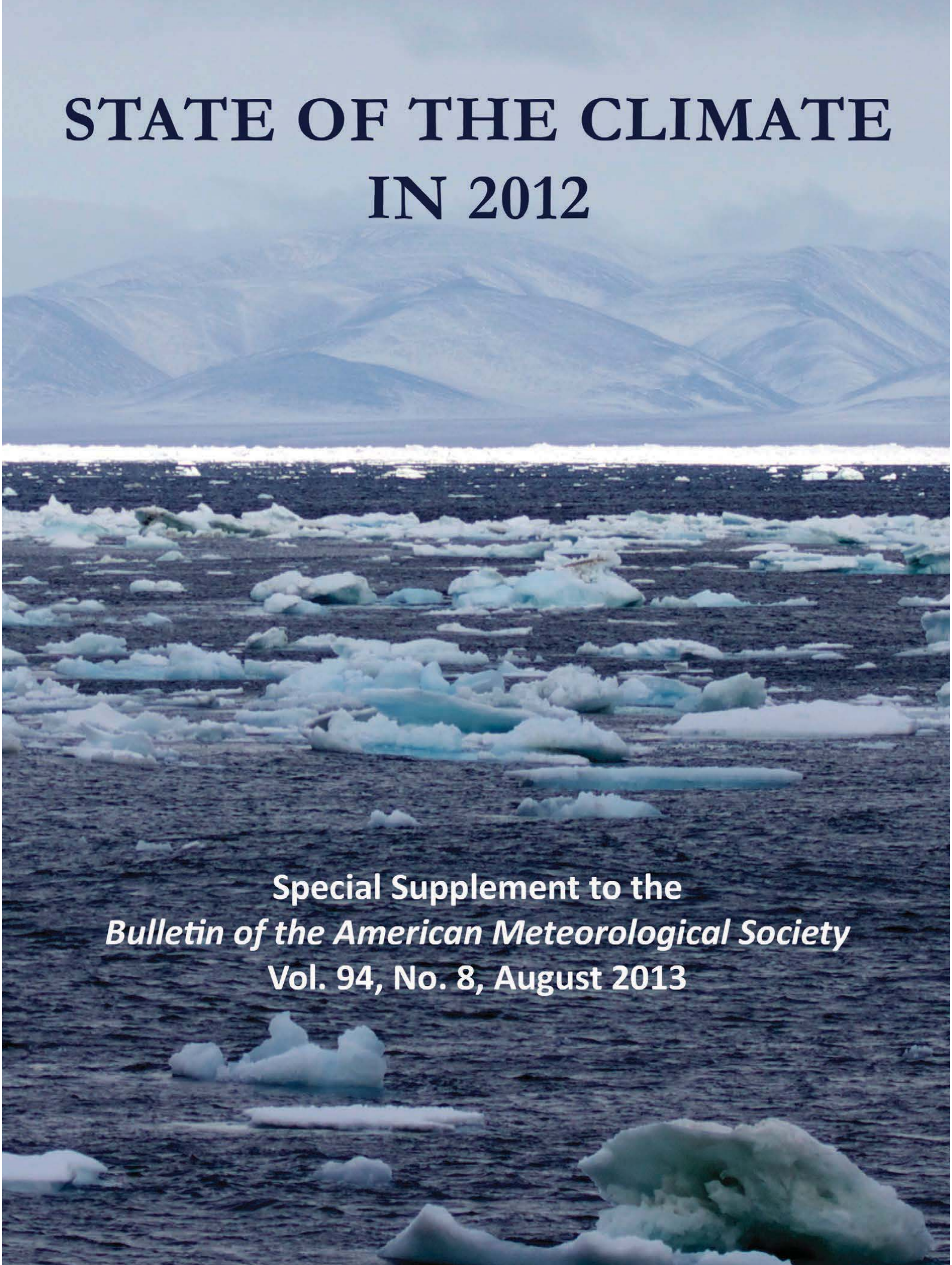

Special Supplement to the
Bulletin of the American Meteorological Society
Vol. 94, No. 8, August 2013

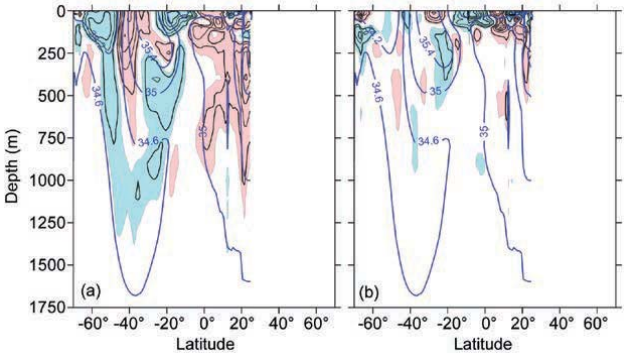

Fig. 3.16. Zonally averaged (a) 2012 salinity anomaly and (b) 2012 minus 2011 salinity field for the Indian Ocean. Blue shading represents negative (fresh) anomalies <-0.01, red shading represents positive (salty) anomalies >0.01. The contour interval for the anomalies is 0.02. In the background of each figure (thick blue contours) is the zonally-averaged climatological mean salinity (WOA09). Contour intervals for the background are 0.4. All values are on the PSS.

ceeding 700 m. From 2011 to 2012, changes exceeding 0.02 in the North Indian Ocean were mainly confined to the upper 150-m depth. This includes a freshening about the equator and positive/salty anomaly to the north. This salty anomaly in the upper 100-m depth (not shown, but closely resembles Fig. 3.11b) exceeds 0.02 in the eastern North Indian Ocean, while smaller and of opposite sign in the western North Indian. The eastern Arabian Sea is saltier in 2012 than 2011, while the western Arabian Sea is fresher. The northeast Bay of Bengal is fresher in 2012 than 2011, as is the area southeast of India, while the central Bay is saltier than 2011.

g. Surface currents—R. Lumpkin, G. Goni, and K. Dohan

This section describes ocean surface current changes, transports derived from ocean surface currents, and features such as rings inferred from surface currents. Surface currents are obtained from in situ (global array of drogued drifters and moorings) and satellite (altimetry, wind stress, and SST) observations. Transports are derived from a combination of sea height anomaly (from altimetry) and climatological hydrography. See previous *State of the Climate* reports for details of these calculations Global zonal current anomalies and changes in anomalies from 2011 are shown in Fig. 3.17 and discussed below for individual ocean basins.

1) Pacific Ocean

In the tropical Pacific, 2012 began with equatorial currents exhibiting ~20 cm s^{-1} westward anomalies in the longitude band 100°W–160°W, a strengthening of the climatological January westward current on the equator. In the same longitude band, eastward anomalies of ~10 cm s^{-1} at 10°N indicated that the North Equatorial Countercurrent had shifted slightly north of its climatological January location of 6°N–7°N. By February, this situation had changed dramatically as eastward anomalies of 20 cm s^{-1}–30 cm s^{-1} developed in the region 4°S–5°N, 100°W–140°W. Weaker eastward anomalies were also present between this region and the dateline, on and north of the equator. By March, the eastward anomalies dominated the entire basin from 5°S to 10°N, with peak anomalies of ~35 cm s^{-1} on the equator between 110°W and 140°W. This pattern continued to intensify in April, when strong eastward anomalies exceeding 40 cm s^{-1} were present across the equatorial Pacific. These strong eastward anomalies advected warm water into the central equatorial Pacific, erasing the negative SST anomalies associated with the La Niña conditions that had persisted there since the previous year (see section 3b).

By May, the eastward anomalies across most of the basin had weakened to 20 cm s^{-1}–30 cm s^{-1}, with eastward anomalies exceeding 40 cm s^{-1} persisting between 90°W and 130°W. Weak westward current anomalies began to develop in June at 160°E–180° to disrupt this pattern. During June–August, the region of eastward anomalies shifted westward, perhaps related to the evolution of the discharge-recharge oscillator (Jin 1997) during this period. By August, the region was at 175°E–145°W, with magnitudes still slightly exceeding 40 cm s^{-1}.

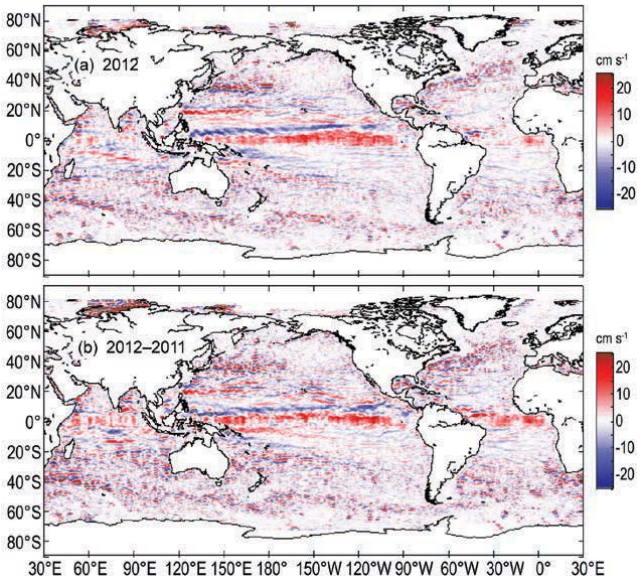

Fig. 3.17. Global zonal geostrophic anomalies for (a) 2012 and (b) 2012 minus 2011, in cm s^{-1}, derived from a synthesis of drifters, altimetry, and winds.

Tropical Pacific anomalies changed significantly in September 2012; the region of eastward anomalies diminished rapidly in size and magnitude as it shifted to 160°E–180°, and westward anomalies of about -20 cm s^{-1} (negative=westward) developed on the equator from 120°W to 180°. North of this band of westward anomalies, eastward anomalies of 10 cm s^{-1}–20 cm s^{-1} persisted between 4°N and 6°N until November. Through the remainder of 2012, westward anomalies developed across the equatorial Pacific, reaching their maxima in December when these anomalies were present from 160°E to 100°W, peaking at -20 cm s^{-1} on the equator and extending from 6°S to 5°N.

The annual average zonal current anomaly for 2012 in the Pacific (Fig. 3.17, top) was dominated by the strong eastward anomalies that were present during February–August. This pattern is also seen in the 2012–2011 anomaly map (Fig. 3.17, bottom), as 2011 was (in the annual average) a relatively neutral year for surface current anomalies in the tropical Pacific.

Surface current anomalies in the equatorial Pacific typically lead SST anomalies by several months, with a magnitude that scales with the SST anomaly magnitude. Recovery to normal current conditions is also typically seen before SST returns to normal. Thus, current anomalies in this region are valuable predictors of the evolution of SST anomalies and their related climate impacts. This leading nature can be seen in the first principal empirical orthogonal function (EOF) of surface current (SC) anomaly and separately of SST anomaly in the tropical Pacific basin (Fig. 3.18). During the period 1993–2012, the maximum correlation between SC and SST is R=0.68 (±0.03 at 95% confidence level), with SC leading SST by 81 days. In 2012, the most dramatic feature of this mode is the rapid change in the SC anomaly pattern from negative values in late 2011 to positive (El Niño-conducive) values in February 2012. This switch in the sign of the SC coincided with a local minimum of the SST anomaly (Fig. 3.18). Over the next several months, as the SC anomaly remained positive, the SST anomaly pattern increased to positive values and remained positive until September. Late in 2012, both the SC and the SST anomaly pattern decreased and became negative before the end of the year.

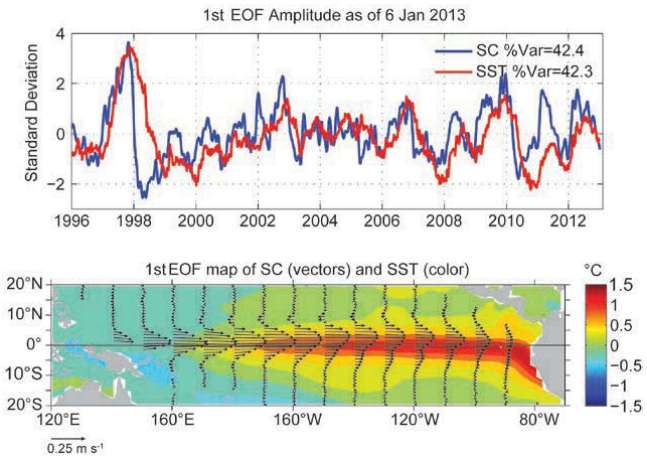

Fig. 3.18. Principal EOF of surface current (SC) and of SST anomaly variations in the tropical Pacific from the OSCAR model. (a) Amplitude time series of the EOFs normalized by their respective standard deviations. (b) Spatial structures of the EOFs.

Since 2010, the Kuroshio has exhibited a narrower and stronger annual mean signature, shifted approximately 1° in latitude to the north compared to 2006–09. This northward shift continued through 2012, with the 2012–2011 zonal current difference (Fig. 3.17b), suggesting that the Kuroshio shifted an additional ~1.5° to the north, from its separation to 175°E. For example, while the climatological latitude of the Kuroshio's core at 150°E is ~34.3°N, the core of the current in 2012 was at ~36.7°N.

2) Indian Ocean

Through the first half of 2012, monthly zonal current anomalies with respect to the climatological monsoon-driven pattern were strong features of the equatorial circulation. In January (the northeast monsoon season), equatorial eastward anomalies of 20 cm s^{-1}–25 cm s^{-1} from the African coast to 70°E, and comparable-magnitude westward anomalies centered on 5°S, indicated a northward shift in the South Equatorial Countercurrent (SECC; Schott and McCreary 2001), which in the climatology is centered on 2.5°S. By February, this pattern had disappeared east of 50°E, with only a remnant remaining in the westernmost basin. The pattern reappeared across much of the basin in March, extending to 85°E but with weaker magnitudes (~15 cm s^{-1} peak anomalies), suggesting a more subtle northward shift of the SECC, and disappeared again in April.

During July–September, the surface current climatology indicates a jet in the Southwest Monsoon Current running from 10°S, 82°E to 14°S, 97°E at 25 cm s^{-1}–30 cm s^{-1} in July and September, peaking at 40 cm s^{-1} in August. As early as March 2012, eastward anomalies were present along the path of this climatological eastward jet, suggesting anomalously early formation. This pattern was pronounced through boreal summer, consistent with a near doubling of the current speed, and persisted through October. This feature dominates the annual mean zonal current anomaly in the Indian Ocean basin (Fig. 3.17).

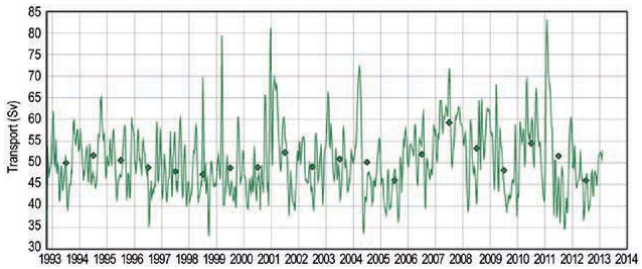

Fig. 3.19. Altimetry-derived transport of the Agulhas Current from a combination of sea height anomaly and climatological hydrography. (Source: http://www.aoml.noaa.gov/phod/altimetry/cvar/agu/index.php.)

The altimetry-derived annual mean transport of the Agulhas Current (Fig. 3.19) decreased abruptly in mid-2011 compared to its long-term mean; this reduced transport persisted in 2012 when the annual mean Agulhas transport was ~46 Sv (1 Sv = 1×10^6 m^3 s^{-1}) , which (along with 2005) was the lowest annual mean observed since the beginning of the altimetric record in 1993. Despite this decreased transport, the number of eddies shed from the Agulhas retroflection into the Atlantic basin remained at its climatological average (5–7 rings per year) as observed from satellite altimetry.

3) Atlantic Ocean

In January 2012 the tropical Atlantic did not exhibit any basin-scale surface current anomalies. This changed across the basin in February, when strong (20 cm s^{-1}–35 cm s^{-1}) eastward anomalies were seen from 40°W to 10°E (the African coast) between 4°S and 4°N, with the strongest anomalies in the band 0°–10°W. These eastward anomalies weakened in March and were seen only in two relatively narrow longitude bands (22°W–30°W and 4°W–10°W) in April. In May–June, large-scale eastward equatorial anomalies persisted east of 30°W, while westward anomalies developed in the western basin immediately north of the equator. In June, strong westward anomalies of -40 cm s^{-1} were seen at 1°N–2°N, 34°W–42°W, along the northern edge of the climatological North Brazil Current (NBC). In July, these westward anomalies persisted while a band of 20 cm s^{-1}–30 cm s^{-1} eastward anomalies developed at 4°N–5°N, 32°W–46°W along the path of the NBC retroflection/return current and the westernmost North Equatorial Countercurrent (NECC). These alternating bands of westward and eastward anomalies indicated increased shear between the NBC and its return current in the western tropical Atlantic. By August, eastward anomalies associated with the NECC extended from 45°W to 20°W, with a band of westward anomalies north of the eastward anomalies, indicating that the NECC had shifted south of its climatological position. This pattern persisted through the remainder of the year west of ~35°W, while conditions returned to their climatological mean in the interior and eastern tropical Atlantic in September–December.

Along the Gulf Stream pathway in the North Atlantic, alternating bands of eastward (on the north side) and westward (south side) anomalies were present from Cape Hatteras to 45°W. This pattern indicates that the Gulf Stream had shifted 1°–1.5° north of its climatological position in this longitude band. Integrated over both the eastward and westward anomaly regions along the Gulf Stream path, there was no evidence of a significant decrease of the current's annual mean speed in 2012; the overall mean anomaly was -1.2 cm s^{-1} (westward) with a standard deviation of 13.1 cm s^{-1}. This is consistent with transport measurements of the Florida Current, which showed only a minute increase in its annual transport from the 2011 mean (see section 3h).

In the Gulf of Mexico, current anomalies suggest that the Loop Current was weaker or less stable in 2012 than in 2011, with a signature penetrating less far north into the Gulf than in 2011. As noted above, annual-averaged transport of the Florida Current did not change significantly, suggesting that increased variability in 2012 relative to 2011 caused the Loop Current to appear weaker in the 2012 mean. Altimetry-derived estimates of the Yucatan Current indicate that the mean annual transport during 2012 had an above-average value and was close to its largest historical mean of ~29 Sv (http://www.aoml.noaa.gov/phod/altimetry/cvar/yuc/transport.php).

The NBC, which sheds rings that carry waters from the Southern Hemisphere into the North Atlantic basin, exhibited an annual transport and ring shedding close to climatological (since 1993) values. Sea height anomalies in the region, which have generally increased since 2001, continued exhibiting values higher than average in 2012 (Fig. 3.20).

In the southwest Atlantic Ocean, the separation of the Confluence front from the continental shelf break continued to exhibit annual periodicity driven by wind stress curl variations (Goni and Wainer 2001). The annual mean position of the front in 2012 was 38.0°S, a shift to the north of approximately 0.5° latitude from its 2011 location, but still remaining south of its long-term climatological annual mean position of 37.5°S (c.f., Lumpkin and Garzoli 2010; Goni et al. 2011).

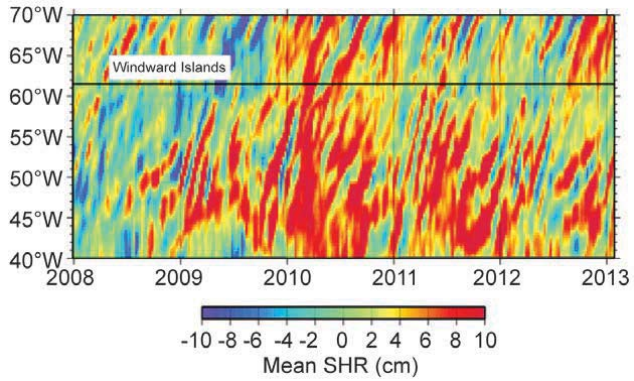

Fig. 3.20. Space-time diagram of deseasoned sea height anomaly (SHR) values along the NBC ring corridor during 2008–12. (Source: http://www.aoml.noaa.gov/phod/altimetry/cvar/nbc.)

h. Meridional overturning circulation and heat transport observations in the Atlantic Ocean—M. O. Baringer, W. E. Johns, G. McCarthy, J. Willis, S. Garzoli, M. Lankhorst, C. S. Meinen, U. Send, W. R. Hobbs, S. A. Cunningham, D. Rayner, D. A. Smeed, T. O. Kanzow, P. Heimbach, E. Frajka-Williams, A. Macdonald, S. Dong, and J. Marotzke

The meridional overturning circulation (MOC) is typically defined as the maximum of the zonally-integrated mass transport stream function. In the Atlantic Ocean the MOC is the large-scale circulation that transports warm near-surface water northward, thereby transferring heat to the atmosphere and returning southward as colder, denser, deeper water. The actual flows are more complicated than this simple description and for further details the reader should see previous *State of the Climate* reports (e.g., Baringer et al. 2011, 2012) or the recent reviews of Srokosz et al. (2012) or Lozier (2012).

The longest time series of a major ocean current contributing to the strength of the MOC is NOAA's Florida Current (FC) data, which began continuous daily measurements in 1982. The full record (Fig. 3.21) shows substantial variability on all measured time scales (Meinen et al. 2010; Baringer and Larsen 2001). The 1982–2012 median transport of daily values is 32.0 ± 0.27 Sv (standard error of the mean based on an integral time scale of about 20 days) with a minimal downward trend of -0.23 ± 0.06 Sv decade^{-1} (90% confidence). In 2012 the annual median was 31.6 ± 1.5 Sv, with the annual mean transport slightly below the average since 2007 (Baringer et al. 2012). However, the 2012 median is within the middle 50% of all annual means. The 2012 daily values of FC transport do show some unusual periods. The daily FC transport values as compared to all previous years (Fig. 3.21, top) indicate that 2012 was unusual in that there were several low transport values (LTP) starting 27 October and ending 24 November. The lowest transport observed occurred on 28 October, reaching only 17.2 Sv. This low value is similar to the lowest transport recorded since 1982 (17.3 Sv on 3 October 1983). The 2012 LTP was preceded by the only high transport event during 2012 that exceeded the 95% confidence limits. This transport exceeded 38 Sv from 3 to 4 October. Low values in the October–November time frame are consistent with the average annual cycle of FC transport (e.g., Meinen et al. 2010). In the last week of October low values are consistent with the passage of Hurricane Sandy northward offshore of the US East Coast. Previous studies have shown that southerly along-shore wind stress can cause a reduction in FC strength, leading to increased sea level along the coast (e.g., Ezer et al. 2013; Sweet et al. 2009). Ezer et al. (2013) quantified this effect using

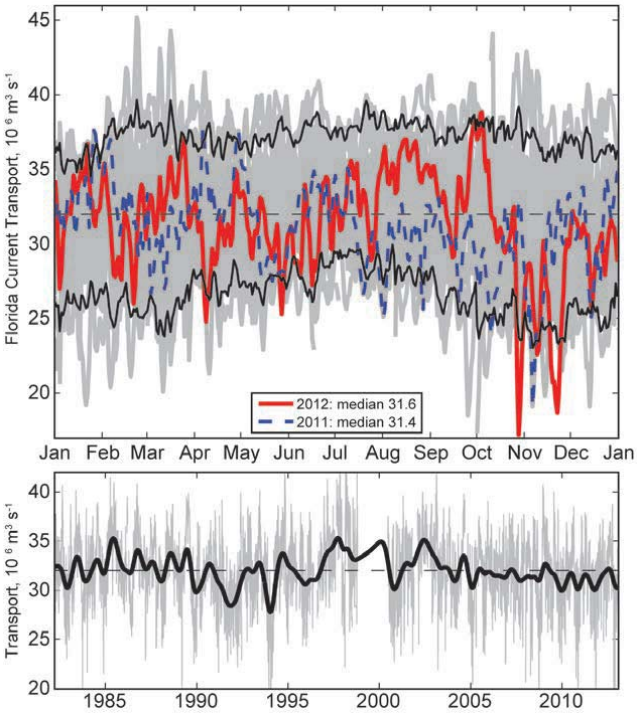

Fig. 3.21. (a) Daily estimates of the transport of the Florida Current during 2012 (red solid line) compared to 2011 (dashed blue line). The daily values of the Florida Current transport for other years since 1982 are shown in light gray and the 95% confidence interval of daily transport values computed from all years is shown in black (solid line); the long-term annual mean is dashed black. The 2012 median transport (31.6 ± 1.5 Sv) lies slightly below the long-term median for the daily values of the Florida Current transport (32.0 Sv). (b) Daily estimates of the Florida Current transport for the full time series record (light gray), and a smoothed version of transport (heavy black line; using a 12-month second-order Butterworth filter) and the mean transport for the full record (dashed black).